Calcium Waves in Agarose Gel with Cell Organelles: Implications of the Velocity Curvature Relationship

Manfred H. P. Wussling,* Kirsten Krannich,* Volker Drygalla,† and Helmut Podhaisky†
*Julius Bernstein Institute of Physiology and †Institute of Numerical Mathematics, Martin Luther University Halle-Wittenberg, D-06097 Halle, Germany

ABSTRACT Calcium oscillations and waves have been observed not only in several types of living cells but also in less complex systems of isolated cell organelles. Here we report the determination of apparent Ca^{2+} diffusion coefficients in a novel excitable medium of agarose gel with homogeneously distributed vesicles of skeletal sarcoplasmic reticulum. Spatio-temporal calcium patterns were visualized by confocal laser scanning fluorescence microscopy. To obtain characteristic parameters of the velocity curvature relationship, namely, apparent diffusion coefficient, velocity of plane calcium waves, and critical radius, positively and negatively curved wave fronts were analyzed. It is demonstrated that gel-immobilized cell organelles reveal features of an excitable medium. Apparent Ca^{2+} diffusion coefficients of the in vitro system, both in the absence or in the presence of mitochondria, were found to be higher than in cardiac myocytes and lower than in unbuffered agarose gel. Plane calcium waves propagated markedly slower in the in vitro system than in rat cardiac myocytes. Whereas mitochondria significantly reduced the apparent Ca^{2+} diffusion coefficient of the in vitro system, propagation velocity and critical size of calcium waves were found to be nearly unchanged. These results suggest that calcium wave propagation depends on the kinetics of calcium release rather than on diffusion.

INTRODUCTION

In several types of excitable and nonexcitable cells, the activation of signal transduction pathways generates calcium oscillations and/or waves. Due to the important impact for cellular function, calcium waves are the subject of intensive experimental and theoretical investigations (Ishide et al., 1990; Lechleiter and Clapham, 1992; Clapham and Sneyd, 1995; Wussling and Salz, 1996; Fontanilla and Nuccitelli, 1998; Gordienko et al., 1998; Keizer et al., 1998; Wagner et al., 1998; Boitier et al., 1999; Boyden et al., 2000; Fink et al., 2000). A presupposition for the development of calcium waves is the existence of an appropriate excitable medium. Spontaneous or stimulated calcium waves in living cells were shown to originate at so-called hot spots with locally increased cytosolic calcium concentration (Cheng et al., 1996; Keizer et al., 1998). Once initiated, regenerative release of calcium from diffusion-coupled sites of the endoplasmic reticulum may propagate a calcium wave. Hence, the mechanism of its spreading is auto-regenerative and consecutive with alternating reaction and diffusion. If the local cytosolic calcium concentration does not increase beyond a critical size, the wave collapses due to the activity of sarco-/endoplasmic reticulum calcium (SERCA) pumps (Clapham, 1995; Misquitta et al., 1999). Both calcium release sites and SERCA pumps are localized in the membranes of the endoplasmic reticulum with slightly varying properties from cell type to cell type (Misquitta et al., 1999). In skeletal or cardiac muscle cells, calcium predominantly is released from ryanodine-sensitive receptors (RyRs 1 and RyRs 2) and taken up again by sarcoplasmic reticulum (SR) Ca-ATPases (Berridge, 1997; Misquitta et al., 1999).

As proven mainly by confocal fluorescence microscopy, calcium dynamics in living cells show general features of excitation waves, namely, asymmetry of the wave profiles (steep increase and flat decay), annihilation after collision (due to refractoriness), dependence of wave speed on the inter-wave period (dispersion relation), and dependence of wave speed on the wave front's curvature (velocity-curvature relationship) (Dockery et al., 1988; Zykov, 1980; Lechleiter et al., 1991; Wussling and Mair, 1999).

There is no doubt that functionally intact mitochondria can modulate the spreading of calcium waves in living cells. An increase of the calcium wave speed was reported to occur in oocytes of *Xenopus laevis* after energization of mitochondria by pyruvate and malate (Jouaville et al., 1995). In rat cortical astrocytes, on the other hand, calcium waves propagated faster after inhibition of the mitochondrial function by antimycin A1 and oligomycin (Boitier et al., 1999). In guinea pig ventricular myocytes, mitochondria are involved in the beat-to-beat regulation of the cytosolic calcium concentration (Isenberg et al., 1993). These effects, however, are most likely due to a close relation between endo/sarcoplasmic reticulum and mitochondria concerning calcium release into and calcium sequestration from the cytosol.

We have recently shown that clusters of vesicles of the SR embedded in agarose gel develop repetitive calcium waves that propagate with lower speed and quite large width in comparison with rat cardiac myocytes (Wussling et al., 1999). There was a clear change of the calcium wave

Received for publication 23 October 2000 and in final form 15 March 2001.

Address reprint requests to Dr. Manfred H. P. Wussling, Martin Luther University Halle-Wittenberg, Julius Bernstein Institute of Physiology, Halle-Wittenberg, Magdeburgerstrasse 6, D-06097 Halle, Germany.

0006-3495/01/06/2658/09 $2.00

patterns after the addition of mitochondria: an increase of the fluorescence intensity accompanied by a higher propagation velocity. The effects could be suppressed by antimycin-A-induced inhibition of the complex III of the respiratory chain. It would appear that numerous findings in the novel in vitro system parallel those of living cells.

To characterize this novel reaction-diffusion system we focused our interest on the velocity-curvature relationship (Zykov, 1980; Keener, 1986; Foerster et al., 1988, 1989; Mikhailov, 1990). One of the advantages of the agarose gel compared with cardiac myocytes or other cells is that spatiotemporal calcium patterns may be observed over a relatively large distance (a few millimeters instead of ~100 μm in rat cardiac myocytes). When positively curved (convex) waves collide, they form cusp-like wave fronts with negative curvature (Foerster et al., 1988; Wussling et al., 1997). Whereas in cardiac cells the assessment of negatively curved (concave) waves is restricted to a few microns (because of the cell's width of ~20 μm), there is no such problem in the gel. This improves the accuracy of the determination of the parameters of the velocity-curvature relationship for three-dimensional waves (see Mikhailov, 1990) with slightly curved fronts (see Brazhnik and Tyson, 1999):

$$N = c - D2K, \tag{1}$$

where N is propagation velocity in general, c is velocity of plane waves, K is curvature, and D is apparent diffusion coefficient. $R_{crit} = 1/K_{crit} = 2D/c$ characterizes a sphere's size that must be exceeded to initiate a traveling wave; i.e., $N > 0$. Spheres with $R < R_{crit}$ must collapse. Eq. 1 differs from the two-dimensional case, where K stands instead of $2K$. As reported previously, a rat ventricular cardiocyte was considered to represent a two-dimensional excitable medium (Wussling and Salz, 1996). This assumption appeared justified because of the cardiocyte's brick-like shape with dimensions of ~150 μm in length, 20 μm in width, and 10 μm thickness and a full-width half-maximum (FWHM) of the calcium wave's intensity profile of ~30 μm. In comparison with the thin cells, the agarose gel with embedded cell organelles appears as a relatively thick layer varying between 170 and 300 μm.

This study is aimed to the determination of apparent diffusion coefficients of Ca^{2+} and Ca^{2+} wave velocities in agarose gel with SR vesicles either in the absence or in the presence of mitochondria. A certain numerical effort is required to fit the wave fronts by appropriate curves. To our knowledge, Ca^{2+} diffusion data of similar systems are not yet reported in the literature. Our interest further focuses on the critical size of a just expanding Ca^{2+} wave in the gel. In rat cardiac myocytes, calcium waves were shown to originate from a single Ca^{2+} spark or a group of Ca^{2+} sparks (Cheng et al., 1996). Finally, to interpret our results, the FitzHugh-Nagumo model (see Keener and Sneyd, 1998) will be applied to the novel system.

MATERIALS AND METHODS

Agarose gel system

SR vesicles were isolated from the *Musculi longissimi dorsi* of German landrace pigs as previously described (Mickelson et al., 1986) and stored at −80°C in a suspension with 300 mM sucrose and 10 mM PIPES (30–40 mg of protein/ml). A suspension of 10 μl of SR vesicles was mixed with 10 μl of liquid agarose gel (type VII, low gelling temperature; Sigma, Diesenhofen, Germany) and 4.7 μl of a buffered salt solution. To obtain homogeneously distributed SR vesicles, the medium was resuspended many times at 37°C. From electron micrographs of gel preparations with relatively high density of SR vesicles (~16 mg of protein/ml of gel) we determined both diameter ø of the microsomes and distance d between the centers of the microsomes (mean ± SD, $n = 33$): ø = 172 ± 37 nm; d = 193 ± 53 nm. Assuming a hexagonal arrangement of spherical SR vesicles with ø = d = constant, the share of the spheres amounts to ($\pi/\sqrt{18}$) or ~74%. If ø/d < 1, then the volume that is occupied by SR vesicles decreases by a factor of $(ø/d)^3$. Based on our morphometric data obtained from a preparation with ~16 mg of protein/ml of gel, the volume of the SR vesicles is estimated to occupy a share of ~50%. Accordingly, the density of SR vesicles results in ~190 per μl of specimen.

The final composition of the medium was (mM) variable $CaCl_2$ (see below), 100 KCl, 5 $MgCl_2$, 4 Na_2-ATP, 10 creatine phosphate, 20 PIPES, 0.01 Fluo-3 or Fluo-4, 0.4% agarose gel, pH 7.2. Spatiotemporal calcium patterns occurred only when the total calcium concentration in the medium varied between 0.15 and 0.35 mM (free $[Ca^{2+}]$ in the absence of waves was estimated by ratiometric measurement with Fluo-4 (filter 530 nm) and Fura red (filter 630 nm) and varied between ~1×10^{-8} M and 3×10^{-8} M). An aliquot of 6 μl of the medium was transferred to a cover glass. Mitochondria were prepared from rat hearts according to Gellerich et al. (1987) and used immediately. In the presence of mitochondria (20–35 mg of protein/ml; usually 2 μl added) the composition of the medium was slightly changed due to the addition of malate/glutamate (final concentrations 5 mM/20 mM) and an enhancement of the total calcium concentration (0.5 mM). For calcium stimulation we used either a glass/metal tip or a drop of 1 μl of caffeine solution (10 mM). Drugs were added by pipettes. The preparation was positioned on the stage of an inverting microscope (Olympus, Tokyo, Japan) and investigated at room temperature. For reasons of reproducibility, either a humid chamber was placed over the medium (~300 μm in thickness at the center of the gel) or a second coverslip was used to cover the preparation and to form a planar layer (170 μm in thickness). The duration of the measurement was limited to 20 min.

Confocal laser scanning microscope (CLSM)

Measurements of spatiotemporal calcium patterns were performed by means of a computer-controlled inverted fluorescence CLSM (INSIGHT-PLUS, Meridian Instruments, Okemos, MI). The light of an argon ion laser to and the emitted light from the line-illuminated specimen pass through a cylindrical lens and is reflected by a galvanometer-driven bilateral scan mirror. Due to the scan system of Brakenhoff (see Brakenhoff and Visscher, 1995) the sample rate of frames of 512 × 480 pixels amounts to 100/s. Images were displayed with a frequency of 25 Hz using a cooled CCD camera. The Z-drive accessory provides a computerized control of optical sectioning with a vertical step size of 0.6 μm at minimum. With the exception of Fig. 1, *C* and *D*, all preparations were observed with a LWD 40×/0.55 NA objective (Olympus). Fig. 1, *C* and *D*, was obtained using a 10×/0.25 NA objective (Olympus).

Image processing

Images were saved on videotape and thereafter digitized using a frame grabber board with the software package QuickCapture (Data Translation,

Marlboro, MA) and a Macintosh IIci computer. Additional software for both calculation of wave speed and presentation of images in this paper was IPLab-Spectrum QC (Signal Analytics, Vienna, VA) and National Institutes of Health Image 1.43 (Microsoft, Redmond, WA).

RESULTS

In freshly prepared suspensions of homogeneously distributed SR vesicles in agarose gel, spatiotemporal calcium patterns occured either spontaneously or after stimulation (see methods). Fig. 1 depicts several types of calcium wave patterns in the focal plane of the specimen, e. g. single waves traveling in one direction, circulating waves, and colliding waves which annihilate each other. The observed calcium patterns well agree with features of other excitable or reaction-diffusion systems (Hess, 1997).

Fig. 1, *A* and *B*, shows a snapshot of a single calcium wave, traveling in a planar agarose gel system (*A*) and the corresponding intensity profile with a steep front and flat back (*B*). The width (FWHM), which varied from preparation to preparation in a wide range (from 50 to 200 μm), was greater in the in vitro system compared with rat cardiac myocytes, where FWHM was 30 $\pm$ 7 μm/s (mean $\pm$ SD, n = 16; own observation). The wave's position is determined at half-maximum intensity of the wave front (see

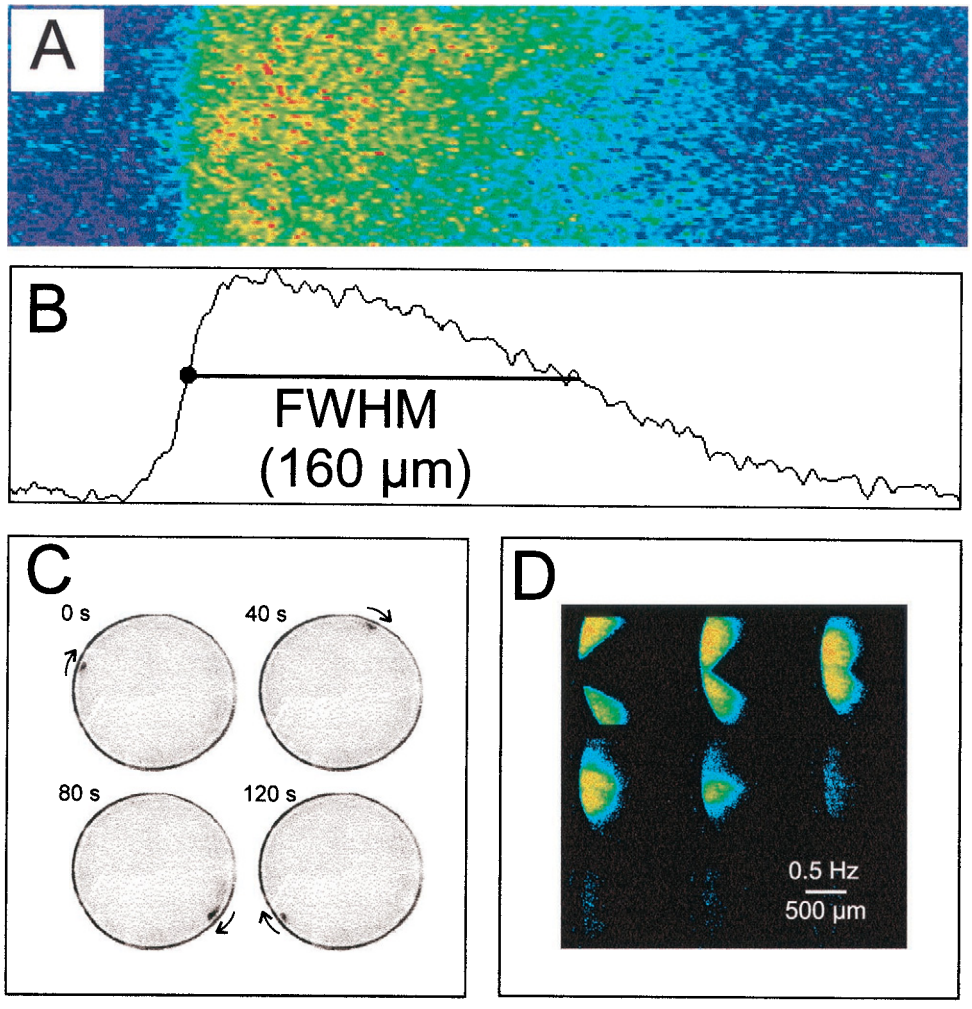

FIGURE 1 Stimulated spatiotemporal calcium patterns in agarose gel with homogeneously distributed vesicles of sarcoplasmic reticulum and Ca^{2+} indicator Fluo-4 (10 μM). (*A* and *B*) Protein concentration, 11.86 mg/ml; total calcium concentration, 0.30 mM. Stimulation was by a metal tip on the edge of the medium. (*A*) Snapshot of a single calcium wave in a selected region of the excitable system (400 μm $\times$ 100 μm). Wave travels from the right to the left with an almost plane front. (*B*) Corresponding intensity profile, showing a steep front and a flat back. Full-width half-maximum (FWHM; see number) was obtained from the whole ROI depicted in *A*. The black dot at half-maximum intensity of the wave front defines the position of the wave. (*C* and *D*) Gel preparation in a humid chamber, no coverslip. Protein concentration was 11.86 mg/ml; total calcium concentration was 0.25 mM. Stimulation was at the boundary of the medium. (*C*) Clockwise circulating calcium wave (see *arrows*) at different moments (0, 40, 80, and 120 s) along a circle with 6.72-mm circumference. Note that the wave prefers the boundary region of the agarose gel. Duration of one revolution was 140 s. Mean propagation velocity was 48 μm/s. Due to the big size of the excitable medium, the picture was composed of several frames. (*D*) Details of two oppositely circulating calcium waves collected at sequential intervals of 2 s. First panel was before or during collision; second panel was collision with gradual annihilation; and third panel was complete annihilation of both waves.

black dot in Fig. 1 *B*). This is important for the determination of velocity, independent of the intensity of fluorescent light or of the gain of the amplifier (see below). When not covered by a second coverslip but located in a humid chamber, circulating calcium waves prefer the boundary region of the gel (Fig. 1, *C* and *D*). This is likely due to an unavoidable effect of evaporation, which causes a higher local calcium concentration in the periphery of the specimen with improved calcium release from the ryanodine receptors of the SR vesicles. Fig. 1 *C* shows a series of images collected at sequential intervals of 40 s of a single calcium wave circulating clockwise (see *arrows*) along a circle with 6.72 mm in circumference. One revolution amounted to 140 s resulting in a propagation velocity of 48 μm/s. Fig. 1 *D*, finally, shows consecutive phases (every 2 s) of two oppositely circulating calcium waves before or during collision (*first panel*), which leads to the wave's gradual (*second panel*) or complete annihilation (*third panel*). Hence, the propagation of calcium waves is not simply due to diffusion or convection but obviously reveals the feature of an excitable medium.

Another important feature of reaction-diffusion systems is the dispersion relation or the dependence of wave speed on the inter-wave period (Dockery et al., 1988). Fig. 2 shows data of an isolated case that was obtained from a cluster of SR vesicles in agarose gel. The fit by a two-phase exponential association makes clear that an undesired influence of the inter-wave period on velocity data is the lower the longer the rest period between the calcium waves is.

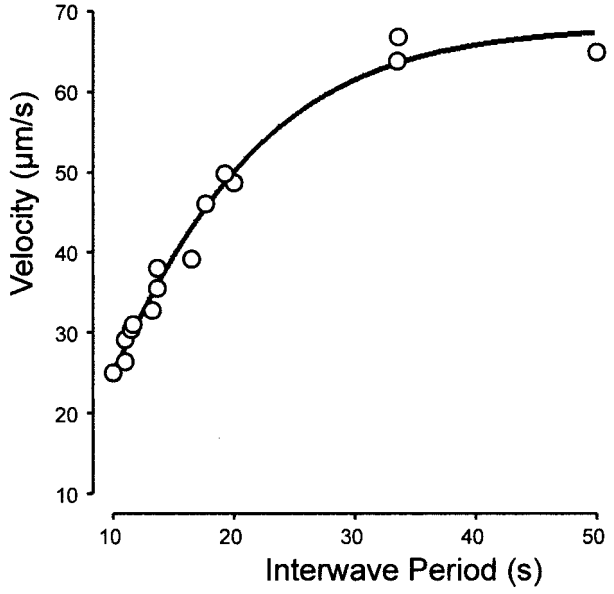

FIGURE 2 Propagation velocity of repetitive plane calcium waves in dependence on the inter-wave period. The plot resulted from a single case investigated in a cluster of SR vesicles (Wussling et al., 1999). Note the lower the inter-wave period the lower the wave speed. This result is predicted by the dispersion relation in excitable media (Dockery et al., 1988).

Under the condition that the rest period before the first calcium wave is sufficiently long (~1 min), it appears to be reasonable to neglect the influence of the inter-wave period on the velocity of the wave spreading throughout the in vitro system. This is of importance for the determination of the velocity curvature relationship.

In the following, we exclusively consider waves that do not travel in the periphery of the agarose gel but that spread throughout it. A single calcium wave usually travels with a positively curved wave front that becomes planar after a sufficiently long distance of propagation (not shown). Occasionally, a couple of waves occurred simultaneously after stimulation. Fig. 3 shows a three-dimensional (*A*) and a two-dimensional (*B*) view of two just colliding calcium waves. A new wave front develops in the collision area that appears cusp-like. To better determine object boundaries at half-maximum fluorescence intensity, the frames were normalized (see example of Fig. 3 *B*).

After determination of the object boundary, the data were plotted, and a set of 100 points around an assumed vertex of the cusp-like wave front (which is considered to be concave or negatively curved) was selected. To determine the minimal negative curvature of the wave front in the area of collision, the boundary points in a small neighborhood of the cusps were approximated by a parabola. This could be done in a manner as described for the case of a double parabola (Wussling et al., 1997).

For our purposes it was sufficient to use the following simplified procedure. Rotate the data points (ξ_i,η_i) by an angle Φ and get (ξ'_i,η'_i). Then the parabola $\eta' = a\xi'^2 + b\xi' + c$ with the parameters a, b, and c for which $F(\Phi) = \Sigma(\eta' - a\xi'^2_i - b\xi'_i - c)^2$ becomes *min*, can be determined explicitly. Therefore, we can find Φ, and in this way the parabola, by solving the one-dimensional minimization problem $F(\Phi)$ becomes *min*.

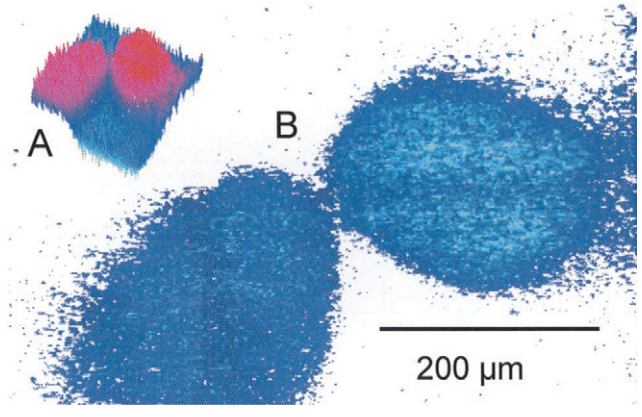

FIGURE 3 Three-dimensional (*A*) and a two-dimensional (*B*) view of two just colliding calcium waves in the agarose gel system. (*A* and *B*) Protein concentration, 12.4 mg/ml; total calcium concentration, 0.35 mM. Waves traveled throughout the gel. Two new wave fronts develop in the collision area that appear cusp-like shaped. To better determine object boundaries at half-maximum fluorescence intensity, the frames were normalized (*B*).

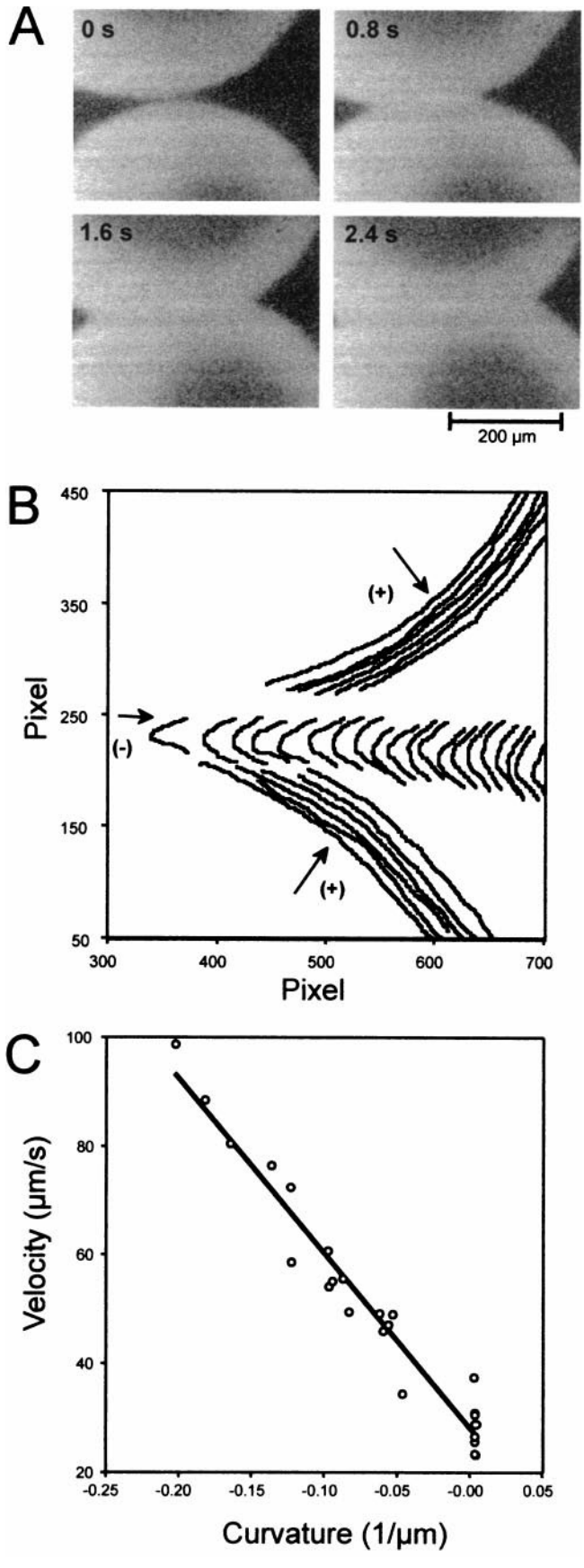

The curvature at the vertex is $-2a$. The velocity was determined via the motion of the vertices of the$_i$,η_i) of the boundaries of the waves before collision were approximated by circles. The problem, $\Sigma[((\xi_i - x_0)^2 + (\eta_i - y_0)^2)^{0.5} - r]^2$ becomes *min,* was solved with respect to (x_0,y_0) (center of circle) and radius r, from which we obtained the curvature $c = r$. The velocity in this case was determined via the distance of the wave fronts (i.e., the average of the minimal distance of each point at time t taken over all points of the wave front at time $t + \Delta t$).

Up to 20 frames (every 200 ms) of one spreading calcium wave were analyzed. The procedure that benefits from the large area of the agarose gel system (5–6 mm in diameter) yields sufficient data of velocity versus curvature to determine the parameters of the velocity-curvature relationship (Eq. 1) relatively accurately.

Details are presented in Fig. 4. The data emerged from a typical preparation of agarose gel with homogeneously suspended SR vesicles. In Fig. 4 *A*, snapshots of two colliding calcium waves are depicted. Fig. 4 *B* shows fragmental calcium wave fronts. The fragments consist of 100 points each (or more) and were selected every 200 ms. Arrows indicate the direction of propagation, the signs (− and +) stand for negative and positive curvature, respectively. Fig. 4 *C* corresponds to Fig. 4 *B* and shows the calculated data of velocity versus curvature, which was fitted by a regression line according to Eq. 1. The example resulted in $D = 151\ \mu m^2/s$, $R_{crit} = 5.8\ \mu m$, and $c = 28.1\ \mu m/s$.

Pooled data of all gel experiments (SR vesicles and SR vesicles plus mitochondria) are plotted in Fig. 5 (top: $n = 18$; bottom: $n = 12$). The comparison of both regression lines shows a stronger negative slope (i.e., a higher apparent diffusion coefficient) in the absence of mitochondria (Fig. 5, top). Mitochondria seem to impair the diffusion conditions as reflected by a flatter regression line (i.e., lower diffusion coefficient) in Fig. 5, bottom.

FIGURE 4 Determination of the velocity curvature relationship from single and colliding calcium waves as observed in a representative preparation of agarose gel with homogeneously suspended SR vesicles. Protein concentration was 16.52 mg/ml; total calcium concentration was 0.15 mM. (*A*) Snapshots of two colliding calcium waves (for time see numbers in the frames). Whereas both single waves are considered positively curved (propagation in vertical direction), wave fronts in the collision region would appear negatively curved (propagation in horizontal direction). Notably, 1) collision does not result in a higher fluorescence intensity in the overlapping zone (not shown here) and 2) the backfronts of the colliding waves almost show a decrease of the fluorescence intensity or the initiation of the wave's annihilation by SERCA pump-induced calcium uptake. (*B*) Corresponding fragmental calcium wave fronts that consist of 100 points each (or more) were selected every 200 ms (scanning of the wave fronts after normalization as shown in Fig. 3 *B*). Direction of propagation is indicated by arrows. The signs (− and +) stand for negative and positive curvature, respectively. (*C*) Data of velocity versus curvature correspond to *B* and were approximated by linear regression according to Eq. 1, resulting in $D = 151\ \mu m^2/s$, $R_{crit} = 5.8\ \mu m$, and $c = 28.1\ \mu m/s$.

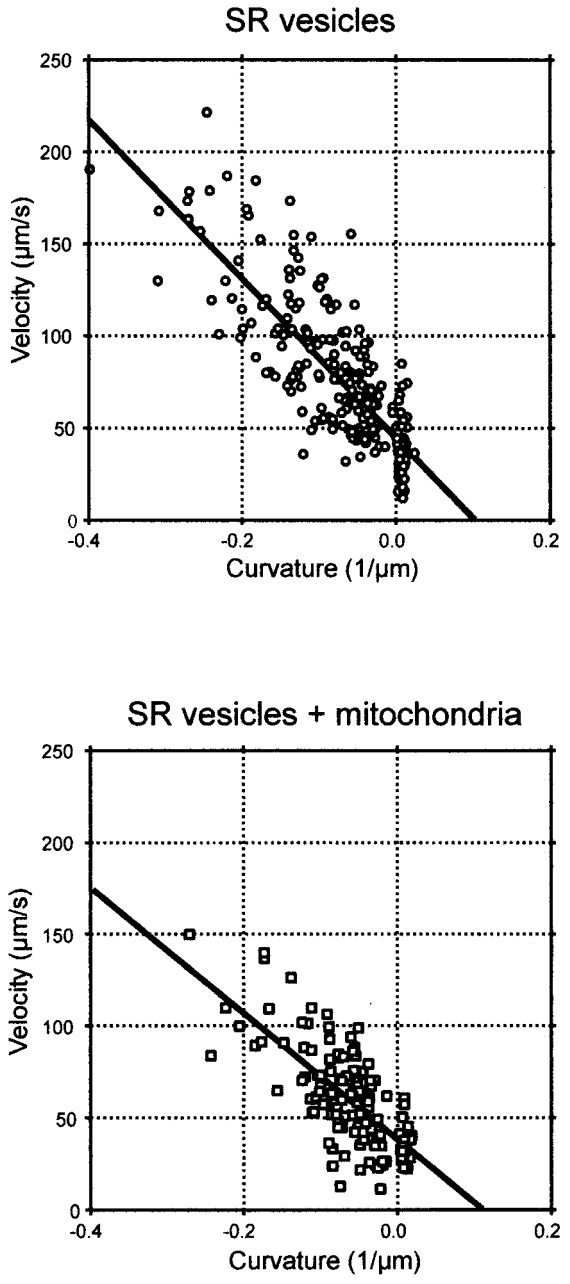

FIGURE 5 Velocity curvature relationship from single and colliding calcium waves as observed in 18 preparations of agarose gel with homogeneously suspended SR vesicles (*top*) and 12 preparations with homogeneously suspended SR vesicles and mitochondria (*bottom*). Note the smaller negative slope (i.e., smaller diffusion coefficient) of regression line in the presence (*bottom*) compared with that in the absence (*top*) of mitochondria. Velocity at zero curvature (i.e., plane waves) and curvature at zero velocity (i.e., no propagating wave) appear insignificantly changed in both groups (see Table 1).

All calculated parameters (mean ± SD) of the velocity-curvature relationship are listed in Table 1. To compare the data obtained from the in vitro system with those of rat cardiac myocytes, Table 1 was completed by previously reported data (Wussling et al., 1997). Table 1 (bottom) additionally contains the diffusion coefficient of Ca^{2+} measured in unbuffered agar gel by a different method (Al-Baldawi and Abercrombie, 1995).

TABLE 1 Calculated parameters of the velocity-curvature relationship

	D ($\mu m^2/s$)	c ($\mu m/s$)	R_{crit} (μm)
SR vesicles in agarose gel ($n = 18$)	215.4 ± 75.4	45.7 ± 12.4	11.2 ± 7.1
SR vesicles + mitochondria in agarose gel ($n = 12$)	149.1 ± 84.2	43.0 ± 14.4	8.3 ± 4.7
Isolated rat cardiac myocytes (Wussling et al., 1997)	120.1	85.7	1.4
Agar gel unbuffered (Al-Baldawi and Abercrombie, 1995)	295.0 ± 74.2		

Results are presented as mean ± SD.

Taken together, 1) independent of the absence or presence of mitochondria, the diffusion coefficients of Ca^{2+} were found to be higher in the in vitro system than in cardiac myocytes and lower than in unbuffered agarose gel (no test of significance was done); 2) plane calcium waves propagated markedly slower in the in vitro system than in rat cardiac myocytes (no test of significance was done); 3) mitochondria significantly changed neither wave speed nor critical radius of a just expanding Ca^{2+} wave in the in vitro system with homogeneously distributed SR vesicles ($p > 0.05$); and 4) mitochondria significantly reduced the apparent diffusion coefficient of Ca^{2+} in the in vitro system ($p < 0.05$).

DISCUSSION

Whereas calcium waves are known to occur in various biological systems (Lechleiter and Clapham, 1992; Rooney and Thomas, 1993; for review see Hess, 1997), there is not much literature about spatiotemporal calcium patterns in suspensions of cell organelles. Ichas et al. (1997) demonstrated the occurrence of traveling depolarization and Ca^{2+} waves stimulated by an increase of the local Ca^{2+} concentration in a gel-immobilized mitochondrial suspension. We recently established a novel excitable medium consisting of skeletal SR vesicles with or without mitochondria suspended in agarose gel and demonstrated spatiotemporal calcium patterns (Wussling et al., 1999).

In the present study, the influence of curvature on propagation velocity of calcium waves was investigated. Fol-

lowing Foerster et al. (1988, 1989) as well as Wussling et al. (1997), who investigated colliding waves in several excitable media, apparent diffusion coefficients were determined using the so-called eikonal equation (Eq. 1). To characterize the agarose gel system with embedded cell organelles, three characteristic parameters were determined: 1) the apparent diffusion coefficient D, 2) the velocity of plane waves c, and 3) the critical radius of a focus with enhanced Ca^{2+} concentration R_{crit}, which must be exceeded to initiate a propagating wave. It would appear that the propagation of calcium waves in agarose gel with homogeneously distributed SR vesicles is due to the regenerative release of calcium ions from diffusion-coupled ryanodine receptors. Therefore, diffusion of calcium ions was assumed to be dominant for the propagation velocity of calcium waves. Table 1 (first column) shows that diffusion coefficients for Ca^{2+}, as determined in this study, are generally smaller than those determined in unbuffered 1% agar gel by Ca-sensitive minielectrodes (Al-Baldawi and Abercrombie, 1995). The differences are likely due to different buffer capacities of the compared media.

Comparison of the in vitro system with rat cardiac myocytes

The diffusion coefficients (Table 1, first column) were found to be enhanced in agarose gel preparations with as well as without mitochondria compared with rat cardiac myocytes, whereby D was determined in both excitable media by the same method. Improved diffusion in the agarose gel is likely due to the lack of diffusion obstacles such as contractile apparatus or the cell's nucleus, which was shown to influence the spreading of calcium waves (Ishida et al., 1999), and to a lower buffer capacity compared with the cytosol of cardiocytes. To the contrary, the propagation velocity of plane calcium waves, c, is smaller in both gel preparations (i.e., with or without mitochondria) compared with cardiocytes (see Table 1, second column). Under the conditions that the experimental determination of the diffusion coefficients is correct, these results clearly show that an improvement of the diffusion conditions does not necessarily result in faster propagating plane waves. One rather would expect the opposite.

To satisfactorily solve the apparent contradiction we made use of the FitzHugh-Nagumo model (e.g., Keener and Sneyd, 1998):

$$du/dt = D\Delta u + (1/\varepsilon)u(1 - u)(u - (v + b)/a)$$

$$\text{and } dv/dt = u - v, \quad (2)$$

where variables u and v stand for excitation and recovery, respectively; D is the diffusion coefficient; and a, b, and e are kinetic parameters. Variables and constants are considered to be dimensionless. We solved Eq. 2 in a two-dimensional space using second-order finite differences and an explicit Runge-Kutta method of the order 5(4). Wave speeds and curvatures have been calculated from expanding circularly shaped fronts. In Fig. 6, two calculated curves of velocity versus curvature are depicted, which resulted from positively curved excitation waves assuming two different diffusion coefficients and different kinetic parameters: (*a*) $D = 2$, $a = 0.8$, $b = 0.05$, and $e = 25$; (*b*) $D = 1.5$, $a = 0.8$, $b = 0.03$, and $e = 33.3$. Fig. 6 shows that all values of the wave speed of curve (*a*, *circles*) are located underneath the corresponding values of curve (*b*, *squares*). Taken together, despite a relatively high diffusion coefficient, propagation velocity was found to be relatively low.

From the presented experimental results and simulations, it would appear that the velocity of regenerative calcium signaling (calcium waves) is dominated by the kinetics of ryanodine receptors rather than by the diffusion between them. This opinion does not conflict with single, and multi, RyR channel experiments. Copello et al. (1997) showed that the maximum open probability of cardiac RyRs is almost double, on average, of that of skeletal RyRs (cf. Fig. 8 in Copello et al., 1997). Table 1, on the other hand, shows that calcium waves in cardiac myocytes propagate by ~100% faster than in gel preparations with SR vesicles of skeletal muscle. Because calcium wave propagation is considered as an auto-regenerative process that depends on the local concentration of Ca^{2+} (released in the wave front), the open probability of the included RyRs is expected to significantly influence the spreading of calcium waves.

Following Foerster et al. (1989), who determined the critical size of a just not-collapsing wave in a chemical

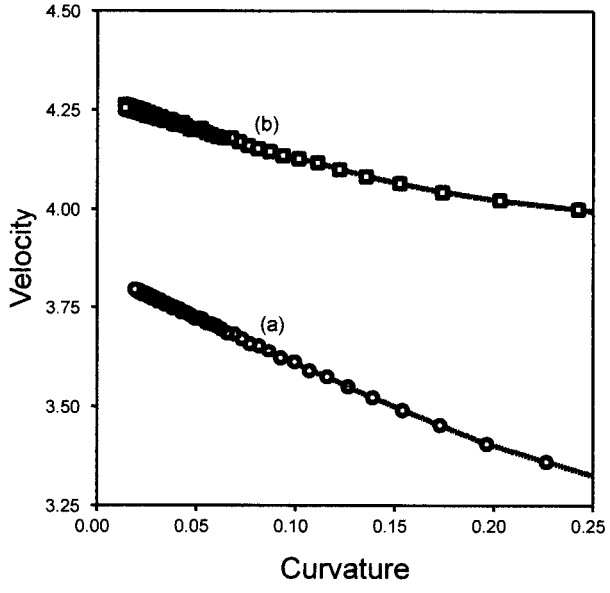

FIGURE 6 Calculated curves of velocity versus curvature using the FitzHugh-Nagumo model (see Eq. 2) with the parameters $D = 2$, $a = 0.8$, $b = 0.05$, and $e = 25$ (*a*, ○) and $D = 1.5$, $a = 0.8$, $b = 0.03$, and $e = 33.3$ (*b*, □). Note smaller values of velocity in curve *a* compared with curve *b* despite higher diffusion coefficient D in *a* compared with *b*.

medium, the so-called critical radius (i.e., 1/critical curvature) results from Eq. 1 when $N = 0$. Unfortunately, there is no direct evidence of R_{crit} of the calcium wave formation, either in the in vitro system or in cardiomyocytes, because an appropriate experimental approach for the excitation of a defined volume was not available to us. We determined the critical curvature by linear regression and extrapolation to the horizontal axis (Fig. 5) and were aware that the critical radii reported in Table 1 are good estimates at best. Nevertheless, due to the fact that R_{crit} was obtained by the same method in both agarose gel with cell organelles (this paper) and cardiac myocytes (Wussling et al., 1997), the comparison of both excitable media appears to be justified. Table 1 (third column) shows higher values of R_{crit} in the gel preparations compared with cardiomyocytes. To speculate, this difference might be due to larger gaps between RyRs of neighboring but separated SR vesicles compared with the more coherent endo/sarcoplasmic reticulum in living cells. Therefore, to reach a critical calcium concentration, the number of diffusion-coupled sites which synchronously release Ca^{2+} and thus the volume of locally enhanced calcium concentration, is expected to be larger in the gel preparations than in cardiac myocytes.

Influence of mitochondria in the in vitro system

The in vitro system can be easily extended by the addition of mitochondria. Because Jouaville et al. (1995) have shown that calcium waves in oocytes of *Xenopus laevis* become accelerated after injection of pyruvate/malate and Falcke et al. (1999) simulated these experimental findings, the interest in the role of mitochondria with respect to intracellular calcium signaling has grown. In rat cortical astrocytes, Boitier et al. (1999) found the opposite, namely, an acceleration of calcium waves after inhibition (by antimycin A 1 and oligomycin) of the mitochondrial Ca^{2+} uptake. The interaction between both mitochondria and endoplasmic reticulum, however, appears to influence Ca^{2+} signaling in various cells in different ways.

From Table 1 (first column), one may find that the extension of the in vitro system through mitochondria leads to a significant decrease of the apparent diffusion coefficient. This is likely due to Ca^{2+} buffering properties of mitochondria, which are expected to reduce the local Ca^{2+} concentration (Duchen, 1999; Boitier et al., 1999). A reduction of the local Ca^{2+} concentration might enhance, diminish, or not affect the calcium-dependent open probability of skeletal ryanodine receptors due to the bell-shaped character of the curve (Copello et al., 1997). We have found that even the propagation velocity of calcium waves in the SR vesicle gel system shows a bell-shaped dependence on the total calcium concentration with a plateau at ~0.25 mM (unpublished results). This observation may explain both an enhancement of propagation velocity (as seen in clusters of cell organelles; Wussling et al., 1999) and a lack of effect of mitochondria on propagation velocity (as found in these experiments with homogeneously distributed cell organelles; Table 1, second column). Interestingly, we did not observe calcium waves in the presence of mitochondria at a total calcium concentration of 0.30 mM. Waves occurred only when the total calcium concentration was enhanced from 0.30 to 0.50 mM and disappeared again after inhibition of the mitochondrial function by antimycin A (unpublished observations). Mitochondria-induced changes of calcium wave speed seem to depend, however, on the density of the cell organelles involved in the generation of calcium waves and on the initial calcium concentration or the corresponding point of the bell-shaped velocity versus calcium relation.

In summary, resuspended vesicles of skeletal sarcoplasmic reticulum in agarose gel exhibit spatiotemporal calcium patterns that underlie the principles of self-organization in excitable media. The velocity-curvature relationship was used to determine apparent diffusion coefficients, velocity of plane waves, and the critical size of a Ca^{2+} hot spot. Plane calcium waves propagated slower in the gel than in rat cardiac myocytes. Apparent diffusion coefficients, to the contrary, were higher in the gel than in rat cardiac myocytes. Mitochondria significantly changed the diffusion coefficient but not the propagation velocity. It may be suggested that regenerative calcium signaling (calcium waves) is dominated by the kinetics of ryanodine receptors rather than by the diffusion between them.

We thank D. Wiedenmann for helping us with the preparation of vesicles of the sarcoplasmic reticulum.

REFERENCES

Al-Baldawi, N. F., and R. F. Abercrombie. 1995. Calcium diffusion coefficient in *Myxicola* axoplasm. *Cell Calcium.* 17:422–430.

Berridge, M. J. 1997. Elementary and global aspects of calcium signalling. *J. Physiol.* 499:291–306.

Boitier, E., R. Rea, and M. R. Duchen. 1999. Mitochondria exert a negative feedback on the propagation of intracellular Ca^{2+} waves in rat cortical astrocytes. *J. Cell Biol.* 145:795–808.

Boyden, P. A., J. Pu, J. Pinto, and H. E. D. J. ter Keurs. 2000. Ca^{2+} transients and Ca^{2+} waves in Purkinje cells: role in action potential initiation. *Circ. Res.* 86:448–455.

Brakenhoff, G. J., and K. Visscher. 1995. Real-time stereo (3D) confocal microscopy. *In* Handbook of Biological Confocal Microscopy. J. B. Pawley, editor. Plenum Press, New York. 355–362.

Brazhnik, P. K., and J. J. Tyson. 1999. Velocity-curvature dependence for chemical waves in the Belousov-Zhabotinsky reaction: theoretical explanations of experimental observations. *Phys. Rev. E.* 59:3920–3925.

Cheng, H., M. R. Lederer, W. J. Lederer, and M. B. Cannell. 1996. Calcium sparks and $[Ca^{2+}]_i$ waves in cardiac myocytes. *Am. J. Physiol. Cell Physiol.* 39:C148–C159.

Clapham, D. E. 1995. Calcium signaling. *Cell.* 80:259–268.

Clapham, D. E., and J. Sneyd. 1995. Intracellular calcium waves. *Adv. Second Messenger Phosphoprotein Res.* 30:1–24.

Copello, J. A., S. Barg, H. Onue, and S. Fleischer. 1997. Heterogeneity of Ca^{2+} gating of skeletal muscle and cardiac ryanodine receptors. *Biophys. J.* 73:141–156.

Dockery, J. D., J. P. Keener, and J. J. Tyson. 1988. Dispersion of traveling waves in the Belousov-Zhabotinskii reaction. *Phys. D.* 30:177–191.

Duchen, M. R. 1999. Contributions of mitochondria to animal physiology: from homeostatic sensor to calcium signalling and cell death. *J. Physiol.* 516:1–17.

Falcke, M., J. L. Hudson, P. Camacho, and J. D. Lechleiter. 1999. Impact of mitochondrial Ca^{2+} cycling on pattern formation and stability. *Biophys. J.* 77:37–44.

Fink, C. C., B. Slepchenko, I. I. Moraru, J. Watras, J. C. Schaff, and L. M. Loew. 2000. An image-based model of calcium waves in differentiated neuroblastoma cells. *Biophys. J.* 79:163–183.

Foerster, P., S. C. Müller, and B. Hess. 1988. Curvature and propagation of chemical waves. *Science.* 241:685–687.

Foerster, P., S. C. Müller, and B. Hess. 1989. Critical size and curvature of wave formation in an excitable chemical medium. *Proc. Natl. Acad. Sci. U.S.A.* 86:6831–6834.

Fontanilla, R. A., and R. Nuccitelli. 1998. Characterization of the sperm-induced calcium wave in *Xenopus* eggs using confocal microscopy. *Biophys. J.* 75:2079–2087.

Gellerich, F. N., M. Schlame, R. Bohnensack, and W. Kunz. 1987. Dynamic compartmentation of adenine nucleotides in the mitochondrial intermembrane space of rat-heart mitochondria. *Biochim. Biophys. Acta.* 890:117–126.

Gordienko, D. V., T. B. Bolton, and M. B. Cannell. 1998. Variability in spontaneous subcellular calcium release in guinea-pig ileum smooth muscle cells. *J. Physiol.* 507:707–720.

Hess, B. 1997. Periodic patterns in biochemical reactions. *Q. Rev. Biophys.* 30:121–176.

Ichas, F., L. S. Jouaville, and J. P. Mazat. 1997. Mitochondria are excitable organelles capable of generating and conveying electrical and calcium signals. *Cell.* 89:1145–1153.

Isenberg, G., S. Han, A. Schiefer, and M.-F. Wendt-Gallitelli. 1993. Changes in mitochondrial calcium concentration during the cardiac contraction cycle. *Cardiovasc. Res.* 27:1800–1809.

Ishida, H., C. Genka, Y. Hiruta, H. Nakazawa, and W. H. Barry. 1999. Formation of planar and spiral Ca^{2+} waves in isolated cardiac myocytes. *Biophys. J.* 77:2114–2122.

Ishide, N., T. Urayama, K. I. Inoue, T. Komaru, and T. Takishima. 1990. Propagation and collision characteristics of calcium waves in rat myocytes. *Am. J. Physiol.* 259:H940–H950.

Jouaville, L. S., F. Ichas, E. L. Holmuhamedov, P. Camacho, and J. D. Lechleiter. 1995. Synchronization of calcium waves by mitochondrial substrates in *Xenopus laevis* oocytes. *Nature.* 377:438–441.

Keener, J. P. 1986. A geometrical theory for spiral waves in excitable media. *S. IA. M. J. Appl. Mathematics.* 46:1039–1056.

Keener, J., and L. Sneyd. 1998. Mathematical Physiology. Springer-Verlag, New York. 136–142.

Keizer, J., G. D. Smith, S. Ponce-Dawson, and J. Pearson. 1998. Saltatory propagation of Ca^{2+} waves by Ca^{2+} sparks. *Biophys. J.* 75:595–600.

Lechleiter, J. D., and D. E. Clapham. 1992. Molecular mechanisms of intracellular calcium excitability in *X. laevis* oocytes. *Cell.* 69:283–294.

Lechleiter, J., S. Girard, E. Peralta, and D. Clapham. 1991. Spiral calcium wave propagation and annihilation in *Xenopus* oocytes. *Science.* 252: 123–126.

Mickelson, J. R., J. A. Ross, B. K. Reed, and C. F. Louis. 1986. Enhanced Ca^{2+}-induced calcium release by isolated sarcoplasmic reticulum vesicles from malignant hyperthermia susceptible pig muscle. *Biochim. Biophys. Acta.* 862:318–328.

Mikhailov, A. S. 1990. Foundations of synergetics. I. Distributed active systems. *Springer Ser. Synerget.* 51:27–28.

Misquitta, C. M., D. P. Mack, and A. K. Grover. 1999. Sarco/endoplasmic reticulum Ca^{2+} (SERCA)-pumps: link to heart beats and calcium waves. *Cell Calcium.* 25:277–290.

Rooney, T. A., and A. P. Thomas. 1993. Intracellular calcium waves generated by Ins(1,4,5)P_3-dependent mechanisms. *Cell Calcium.* 14: 674–690.

Wagner, J., Y.-X. Li, J. Pearson, and J. Keizer. 1998. Simulation of the fertilization Ca^{2+} wave in *Xenopus laevis* eggs. *Biophys. J.* 75: 2088–2097.

Wussling, M. H. P., K. Krannich, G. Landgraf, A. Herrmann-Frank, D. Wiedenmann, F. N. Gellerich, and H. Podhaisky. 1999. Sarcoplasmic reticulum vesicles embedded in agarose gel exhibit propagating calcium waves. *FEBS Lett.* 463:103–109.

Wussling, M., and T. Mair. 1999. Calcium waves in rat cardiac myocytes underlie the principles of self-organization in excitable media. *In* Lecture Notes in Physics, Vol. 532: Transport and Structure: Their Competitive Roles in Biophysics and Chemistry. S. C. Müller, J. Parisi, and W. Zimmermann, editors. Springer, Berlin. 151–163.

Wussling, M. H. P., and H. Salz. 1996. Nonlinear propagation of spherical calcium waves in rat cardiac myocytes. *Biophys. J.* 70:1144–1153.

Wussling, M. H. P., K. Scheufler, S. Schmerling, and V. Drygalla. 1997. Velocity-curvature relationship of colliding spherical calcium waves in rat cardiac myocytes. *Biophys. J.* 73:1232–1242.

Zykov, V. S. 1980. Analytical evaluation of the dependence of the speed of an excitation wave in two-dimensional excitable medium on the curvature of its front. *Biophysics.* 25:906–911.